© 2017. Published by The Company of Biologists Ltd | Journal of Experimental Biology (2017) 220, 531-536 doi:10.1242/jeb.149625

SHORT COMMUNICATION

Right-to-left shunt has modest effects on CO_2 delivery to the gut during digestion, but compromises oxygen delivery

Christian Lind Malte[1,*], Hans Malte[1], Lærke Rønlev Reinholdt[1], Anders Findsen[1], James W. Hicks[2] and Tobias Wang[1]

ABSTRACT

By virtue of their cardiovascular anatomy, reptiles and amphibians can shunt blood away from the pulmonary or systemic circuits, but the functional role of this characteristic trait remains unclear. It has been suggested that right-to-left (R–L) shunt (recirculation of systemic blood within the body) fuels the gastric mucosa with acidified and CO_2-rich blood to facilitate gastric acid secretion during digestion. However, in addition to elevating P_{CO_2}, R–L shunt also reduces arterial O_2 levels and would compromise O_2 delivery during the increased metabolic state of digestion. Conversely, arterial P_{CO_2} can also be elevated by lowering ventilation relative to metabolism (i.e. reducing the air convection requirement, ACR). Based on a mathematical analysis of the relative roles of ACR and R–L shunt on O_2 and CO_2 levels, we predict that ventilatory modifications are much more effective for gastric CO_2 supply with only modest effects on O_2 delivery. Conversely, elevating CO_2 levels by means of R–L shunt would come at a cost of significant reductions in O_2 levels. The different effects of altering ACR and R–L shunt on O_2 and CO_2 levels are explained by the differences in the effective blood capacitance coefficients.

KEY WORDS: Gas exchange, Heart, Mathematical model, Reptile, Shunting

INTRODUCTION

The ability to shunt blood away from the pulmonary or systemic circulations is a defining character of the reptilian and amphibian cardiovascular systems (Hicks, 1998). However, whilst much is known about the anatomical basis for central vascular shunts and their autonomic regulation, the functional role of bypassing one or the other circulation remains as mysterious as it is debated (Hicks and Wang, 2012). Thus, it remains uncertain as to whether this cardiovascular design is an exquisite adaptation to low ectothermic metabolism and intermittent pulmonary ventilation, or merely an atavistic relict with no particular functional benefits (Hicks and Wang, 2012).

In several species of reptiles and amphibians, the right-to-left (R–L) shunts (i.e. the direct recirculation of systemic venous blood into the arterial systemic circulation) decrease whenever oxygen demands are elevated (Hicks and Wang, 2012). However, in crocodilians, an elevated oxygen consumption associated with digestion may be an exception. A combination of unique anatomical features of the crocodilian cardiovascular system (Hicks, 1998) combined with physiological measurements fostered the idea that increased R–L shunts serve to fuel the gastric mucosa with acidic proton-rich blood during digestion in alligators (Farmer et al., 2008; Gardner et al., 2011; Jones and Shelton, 1993). Central to this proposal is the observation that the crocodilian coeliac artery appears as a continuation of the left aortic arch, which indicates that the stomach is preferentially perfused with CO_2-rich blood from the right ventricle (e.g. Jones, 1996; Webb, 1979). In support for elevated (systemic) arterial partial pressure of CO_2 (P_{CO_2}) governing acid secretion, Farmer et al. (2008) reported slower digestion after surgical removal of the left aorta in alligators. However, a number of other studies show that growth is not affected by similar procedures (Eme et al., 2009, 2010), and it is possible that the slower digestion stems from reduced perfusion of the gastrointestinal organs after occlusion of the left aortic arch (Hicks and Wang, 2012).

Although the cardiovascular system must simultaneously provide for O_2 delivery and CO_2 removal, the proposition that R–L shunts assist gastric acid secretion has not included considerations of the inexorable reduction in O_2 delivery. R–L shunts cause large reduction in arterial O_2 levels – whether expressed as partial pressure, O_2 concentration or haemoglobin saturation (Wang and Hicks, 1996) – while the effects on arterial P_{CO_2} are predicted to be considerably smaller given the high capacitance coefficient for CO_2 in blood. An increased R–L shunt during digestion would therefore also compromise O_2 delivery, which seems undesirable given the fourfold elevation in O_2 demands during digestion (Busk et al., 2000). In this context, it may be more prudent to elevate arterial P_{CO_2} by means of ventilation [i.e. a lowering of the air convection requirement (ACR) for CO_2], a response that has been suggested to compensate for the rise in plasma bicarbonate during digestion (the so-called 'alkaline tide'; Hicks et al., 2000; Hicks and White, 1992; Wang et al., 2001b). However, decreasing the ACR to elevate CO_2 levels will simultaneously lower the lung P_{O_2} and could negatively impact O_2 delivery.

To address the compromise between adequate O_2 delivery and arterial acid–base status, we developed an integrated numerical model that can be applied to amphibians and reptiles, to provide a quantitative comparison of the effects of R–L shunting and altered ventilation on blood O_2 and CO_2 levels.

MATERIALS AND METHODS

Fig. 1A illustrates the model of gas exchange for O_2 and CO_2 based on mass balances and relationships that express electro-neutrality in blood compartments. The model does not include diffusion limitations or spatial heterogeneities at tissues or lungs, and incorporates a thermodynamically correct description of the Bohr–Haldane effect.

[1]Zoophysiology, Department of Bioscience, Aarhus University, 8000 Aarhus C, Denmark. [2]Department of Ecology and Evolutionary Biology, University of California, Irvine, CA 92697, USA.

*Author for correspondence (christian.malte@bios.au.dk)

C.L.M., 0000-0002-7003-6370

Received 12 September 2016; Accepted 6 December 2016

Journal of Experimental Biology (2017) 220, 531-536 doi:10.1242/jeb.149625

List of symbols and abbreviations

ACR	air convection requirement
C_{PaCO_2}, C_{PaO_2}	concentration of CO_2 or O_2 in the pulmonary artery
C_{PvCO_2}, C_{PvO_2}	concentration of CO_2 or O_2 in pulmonary venous return (i.e. left atrium)
C_{SaCO_2}, C_{SaO_2}	concentration of CO_2 or O_2 in the systemic arterial blood
C_{SvCO_2}, C_{SvO_2}	concentration of CO_2 or O_2 in systemic venous return (i.e. right atrium)
Hb	haemoglobin
L_{shunt}	gas exchange limitation imposed by shunts
p	number of Bohr-groups of haemoglobin
P_{ACO_2}, P_{AO_2}	partial pressure of CO_2 or O_2 in the lung gas
P_{CO_2}, P_{O_2}	partial pressure of CO_2 or O_2 in a given compartment
P_{ICO_2}, P_{IO_2}	inspired partial pressure of CO_2 or O_2
$\dot{Q}_{LR}$	left-to-right shunt flow
$\dot{Q}_{pul}$	pulmonary blood flow
$\dot{Q}_{RL}$	right-to-left shunt flow
$\dot{Q}_{sys}$	systemic blood flow
$\dot{Q}_{tot}$	total cardiac output
R–L	right-to-left shunt
R_{perf}	blood convective/perfusive resistance
RQ	respiratory quotient
R_{tot}	total resistance imposed to transport between tissues and the environment
R_{vent}	air convective/ventilatory resistance
S_H	fractional saturation of haemoglobin with protons
S_{O_2}	HbO_2 saturation
λ	blood/gas partitioning coefficient

Mass balances

For O_2:

$$\dot{V}_{O_2} = \dot{Q}_{sys}(C_{SaO_2} - C_{SvO_2}), \quad (1)$$

$$\dot{Q}_{pul}C_{PvO_2} + \dot{Q}_{RL}C_{PaO_2} = \dot{Q}_{sys}C_{SaO_2} + \dot{Q}_{LR}C_{SaO_2}, \quad (2)$$

$$\dot{Q}_{sys}C_{SvO_2} + \dot{Q}_{LR}C_{SaO_2} = \dot{Q}_{RL}C_{PaO_2} + \dot{Q}_{pul}C_{PaO_2}, \quad (3)$$

$$\dot{V}_A\beta_g(P_{IO_2} - P_{AO_2}) = \dot{Q}_{pul}(C_{PvO_2} - C_{PaO_2}). \quad (4)$$

For CO_2:

$$\dot{V}_{CO_2} = \dot{Q}_{sys}(C_{SvCO_2} - C_{SaCO_2}), \quad (5)$$

$$\dot{Q}_{pul}C_{PvCO_2} + \dot{Q}_{RL}C_{PaCO_2} = \dot{Q}_{sys}C_{SaCO_2} + \dot{Q}_{LR}C_{SaCO_2}, \quad (6)$$

$$\dot{Q}_{sys}C_{SvCO_2} + \dot{Q}_{LR}C_{SaCO_2} = \dot{Q}_{RL}C_{PaCO_2} + \dot{Q}_{pul}C_{PaCO_2}, \quad (7)$$

$$\dot{V}_A\beta_g(P_{ACO_2} - P_{ICO_2}) = \dot{Q}_{pul}(C_{PaCO_2} - C_{PvCO_2}). \quad (8)$$

See Table 1 and the list of symbols and abbreviations for parameter definitions.

Concentrations and partial pressures in blood

The concentration of O_2 in each blood compartment (C_{bO_2}) is the sum of haemoglobin (Hb)-bound O_2 [product of blood Hb concentration (C_{Hb}), number of O_2 binding sites (q=4) and saturation (S_{O_2})] and the physically dissolved O_2 [product of physical solubility (α_{O_2}) and P_{O_2}]:

$$C_{bO_2} = q\,C_{Hb}S_{O_2} + P_{O_2}\alpha_{O_2}. \quad (9)$$

To quantify the saturation of Hb with O_2 and protons, the Monod–Wyman–Changeux two-state model (Monod et al., 1965) was incorporated where saturation is a function of both P_{O_2} and proton concentration to include the Bohr–Haldane effect.

The total concentration of CO_2 in blood (C_{bCO_2}) is the sum of the physically dissolved CO_2 ($\alpha_{CO_2}P_{CO_2}$) and the bicarbonate and carbonate concentration, as quantified by the equilibrium constants of CO_2 hydration (K_1 and K_2) and the proton concentration ([H^+], which is related to S_{O_2}):

$$C_{bCO_2} = \alpha_{CO_2}P_{CO_2}\left(1 + \frac{K_1}{[H^+]} + \frac{K_1K_2}{[H^+]^2}\right). \quad (10)$$

Electro-neutrality in blood

Equations that express electro-neutrality were derived by conservation of charge, where electro-neutrality in a given blood compartment (subscript i) is given below:

$$[H^+]_i + SID = \frac{K_w}{[H^+]_i} + \alpha_{CO_2}P_{CO_{2i}}\left(\frac{K_1}{[H^+]_i} + \frac{2K_1K_2}{[H^+]_i^2}\right) + \beta_{NB}(\log(1/[H^+]_i) - pH_{iso}) - p\,C_{Hb}S_{Hi}, \quad (11)$$

where SID is the strong-ion difference (Stewart, 1978), K_w is the ionic product of water, β_{NB} is the non-bicarbonate buffer capacity, pH_{iso} is the pH of zero net charge of the buffer groups, S_H is the fractional saturation of haemoglobin with protons and p is the number of Bohr-groups of haemoglobin.

Shunt fractions and blood flows

Total cardiac output ($\dot{Q}_{tot}$) is the sum of pulmonary and systemic flows ($\dot{Q}_{pul}$ and $\dot{Q}_{sys}$, respectively) and the shunt flows ($\dot{Q}_{RL}$ and $\dot{Q}_{LR}$) are given by total blood flow and the shunt fractions ($F_{RL} = \dot{Q}_{RL}/\dot{Q}_{sys}$ and $F_{LR} = \dot{Q}_{LR}/\dot{Q}_{pul}$). Given the desired general applicability of the model to reptiles with (both R–L and L–R) intracardiac shunts, and not just crocodilians with central vascular (R–L) shunts, we derived the following expressions by mass balance, assuming uniformly well-stirred compartments with constant volume where bi-directional shunts can occur independently:

$$\dot{Q}_{pul} = \dot{Q}_{tot}\frac{1 - F_{RL}}{2 - F_{RL} - F_{LR}}, \quad (12)$$

$$\dot{Q}_{sys} = \dot{Q}_{tot}\left(1 - \frac{1 - F_{RL}}{2 - F_{RL} - F_{LR}}\right). \quad (13)$$

However, given the present purpose we only considered unidirectional R–L shunts.

Numerical and analytical solutions

Owing to the simplifying assumptions of the model, at steady-state the pulmonary venous partial pressures of O_2 and CO_2 (P_{PvO_2} and P_{PvCO_2}) are equal to the partial pressures in the lung (P_{AO_2} and P_{ACO_2}). The total system of 12 equations that express mass balance and electro-neutrality with 12 dependent variables (i.e. partial pressures and proton concentrations in the systemic and pulmonary arterial and venous system for O_2 and CO_2) was solved numerically in Mathematica (v.10.3, Wolfram Research).

When blood capacitances of O_2 and CO_2 are assumed constant (approximately true for CO_2 and applicable to O_2 during hypoxia), the system of equations can be solved analytically, leading to the following solutions:

$$\dot{V}_{O_2}R_{tot} = P_{IO_2} - P_{SvO_2}, \quad (14)$$

$$\dot{V}_{CO_2}R_{tot} = P_{SvCO_2} - P_{ICO_2}, \quad (15)$$

where R_{tot} is the total resistance imposed to transport from the blood/tissues to the environment equal to the sum of the resistances

Journal of Experimental Biology (2017) 220, 531-536 doi:10.1242/jeb.149625

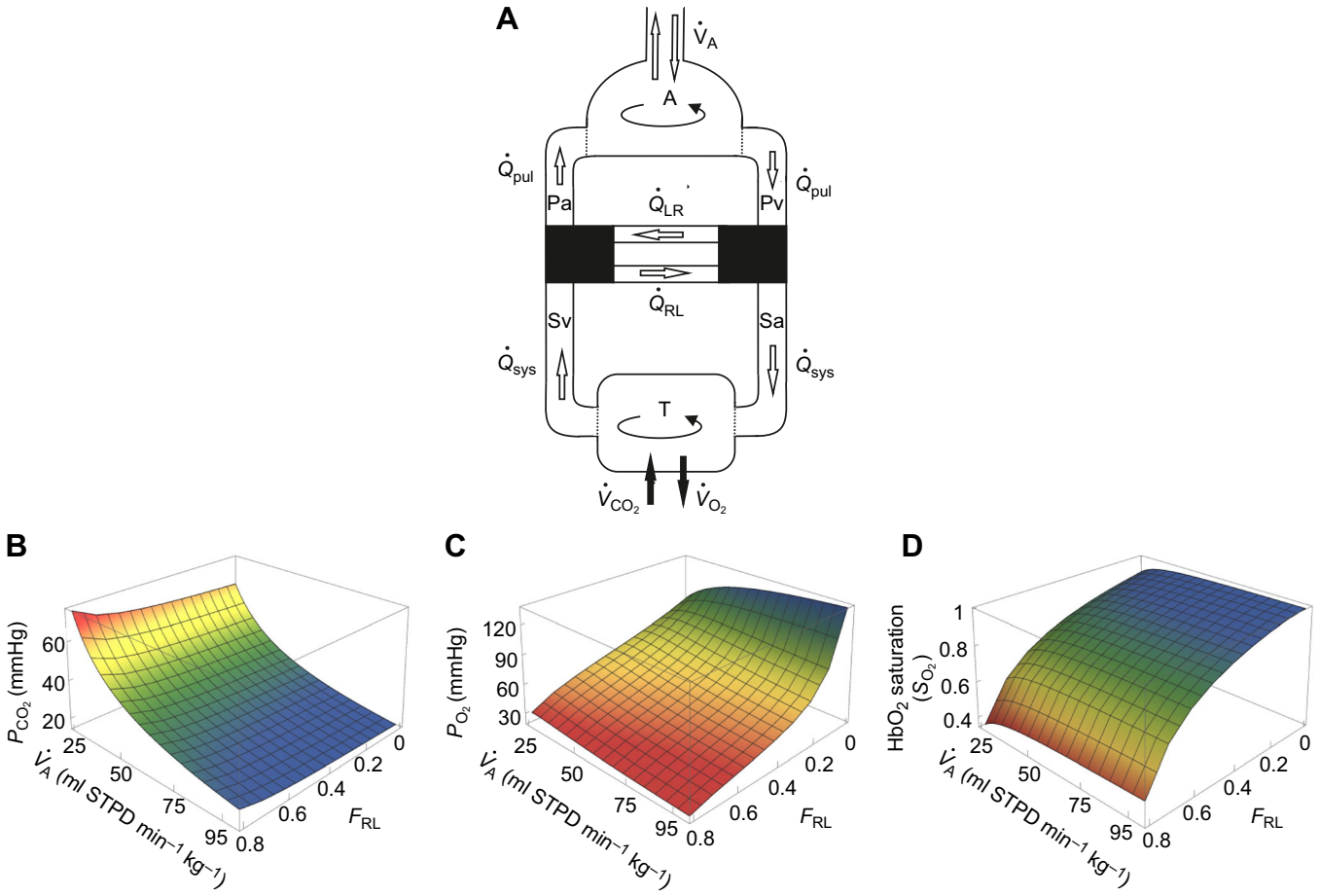

Fig. 1. Model illustration and 3D plots showing the effects of alveolar ventilation (and hence ACR) and F_{RL} on P_{CO_2}, P_{O_2} and S_{O_2}. (A) Illustration of the compartment model with abbreviations as follows: A, lung; Pa, pulmonary arterial blood; Pv, pulmonary venous blood; Sa, systemic arterial blood; Sv, systemic venous blood; T, tissues. For other definitions, see the List of symbols and abbreviations and Table 1. (B–D) 3D plots illustrate how (systemic) arterial P_{CO_2} (B), P_{O_2} (C) and HbO_2 saturation (S_{O_2}; D) change as a function of the alveolar ventilation (and hence air convection requirement, ACR) and the right-to-left shunt fraction (F_{RL}).

associated with blood convective/perfusive transport (R_{perf}) and ventilation (R_{vent}):

$$R_{tot} = R_{perf} + R_{vent}. \quad (16)$$

When only considering unidirectional R–L shunts, the total resistance simplifies to:

$$R_{tot} = \frac{2 - F_{RL}}{\dot{Q}_{tot}\beta_b(1 - F_{RL})} + \frac{1}{\dot{V}_A\beta_g}, \quad (17)$$

Table 1. Parameter values used in simulations

Parameters and variables	Abbreviation	Value	Reference/notes
Mean alveolar/effective ventilation	$\dot{V}_A$	Varied: 25–100 ml STPD min^{-1} kg^{-1}	
Lung air capacitance coefficient	β_g	1/730 ml STPD ml^{-1} mmHg^{-1}	
Total cardiac output	$\dot{Q}_{tot}$	150 ml min^{-1} kg^{-1}	
Right-to-left shunt fraction	F_{RL}	Varied: 0.0–0.8	
Left-to-right shunt fraction	F_{LR}	0	
Blood non-bicarbonate buffer capacity excluding the contribution from Hb Bohr-groups	β_{NB}	10.08 mmol l^{-1}/pH unit	Leads to similar total non-bicarbonate buffer capacity as reported for turtles (Weinstein et al., 1986)
Strong ion difference	SID	11.42 mmol l^{-1}	Value required for initial condition of P_{CO_2}=35 mmHg, P_{O_2}=100 mmHg, pH=7.2
Haemoglobin concentration	C_{Hb}	1.25 mmol l^{-1}	Half of typical human value
Midpoint for pK	pK_m	7.3	Similar to human value
Isoelectric pH value for haemoglobin	pH_{iso}	7.2	Similar to human value
Physical solubility of O_2 in blood	α_{O_2}	0.00125 mmol l^{-1} mmHg^{-1}	Christoforides and Hedley-Whyte, 1969
Physical solubility of CO_2 in blood	α_{CO_2}	0.032135 mmol l^{-1} mmHg^{-1}	Reeves, 1976
CO_2 production and O_2 consumption	$\dot{V}_{CO_2}$, $\dot{V}_{O_2}$	2 ml STPD min^{-1} kg^{-1}	

Journal of Experimental Biology (2017) 220, 531-536 doi:10.1242/jeb.149625

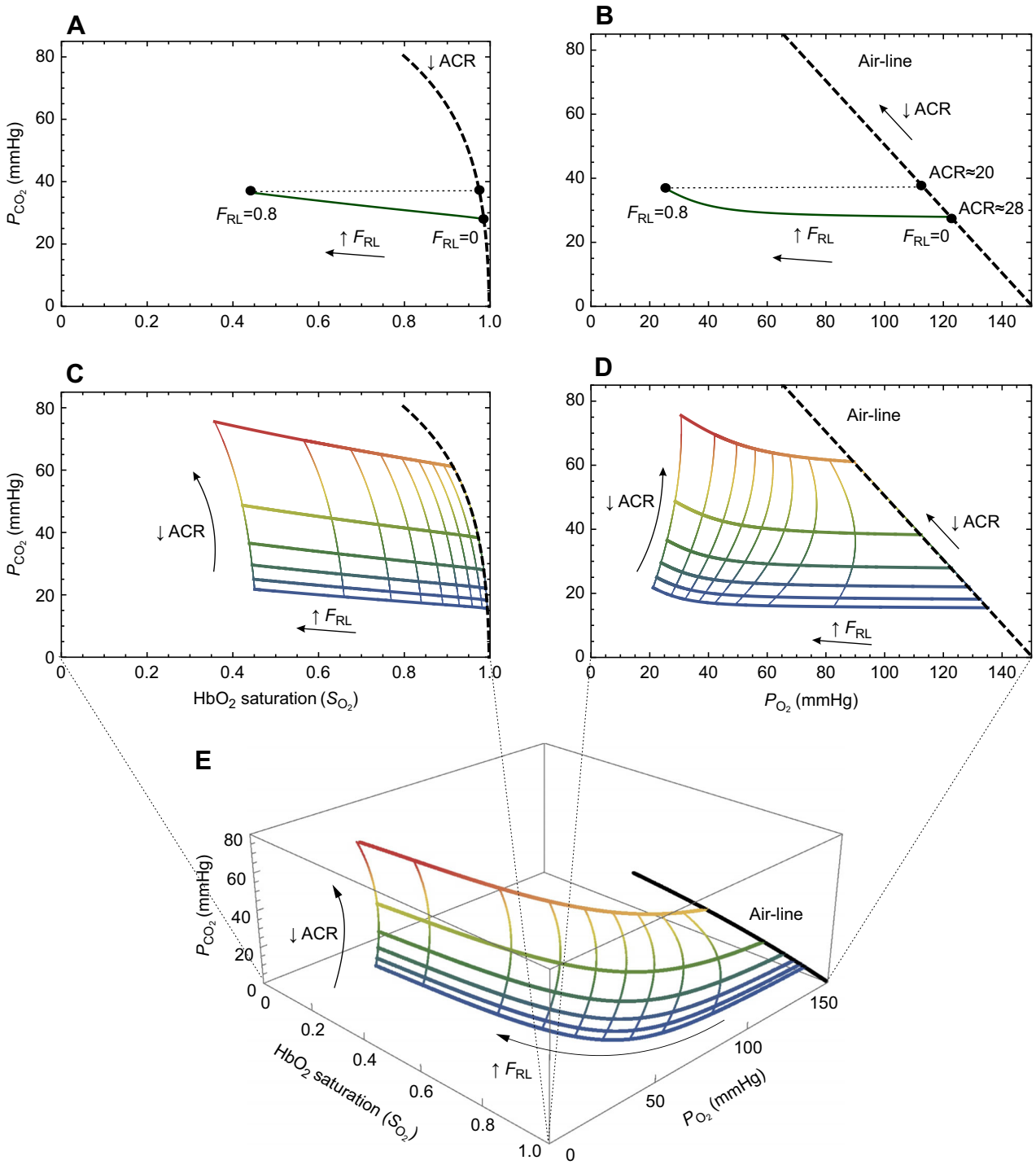

Fig. 2. P_{O_2}–P_{CO_2} diagrams of the solutions comparing the effects of altering ACR and F_{RL} on P_{CO_2}, P_{O_2} and S_{O_2}. (A–D) Arterial P_{CO_2} as a function of either HbO$_2$ saturation (S_{O_2}) (A,C) or P_{O_2} (B,D). In B and D, the dashed black line is the air-line with a slope given by a respiratory quotient (RQ) that describes how P_{CO_2} and P_{O_2} change when altering ACR without shunts, and similarly in A and C, where the 'air-line' becomes a curve. In B, the thick green curve originating at the dashed air-line/curve shows solutions when the right-to-left shunt fraction (F_{RL}) is increased at a constant ACR. Note that to produce the same elevation in arterial P_{CO_2} by means of R–L shunt as by a moderate reduction in ACR (e.g. a reduction from 28 to 20 ml air ml^{-1} CO$_2$), the shunt fraction would have to increase to 0.8 with a concomitant large reduction in arterial P_{O_2} and S_{O_2} (A). (C,D) Solutions for different combinations of F_{RL} (varied 0–0.8) and ACR (varied 12.5–50 ml air ml^{-1} CO$_2$), where the colour coding indicates increasing P_{CO_2}. Here, the thicker curves originating from the air-line/curve show the effects of altering F_{RL} at a given constant ACR. Conversely, the thinner curves originating from the thicker curves show the effects of altering ACR at a given F_{RL}. (E) 3D plot summarizing the effects of altering F_{RL} (thicker curves) and ACR (thinner curves) on both (systemic) venous and arterial blood. The plot is a combination of C and D, where P_{CO_2} is on the vertical *z*-axis and S_{O_2} and P_{O_2} are on the horizontal *x*- and *y*-axes, and therefore also illustrates the effective O$_2$ equilibrium curve. Note that when increasing F_{RL} at a given ACR, the arterial and venous points move down the O$_2$ equilibrium curve with only small elevations in P_{CO_2}. Conversely, reducing ACR at a given shunt leads to pronounced elevations of P_{CO_2} but only moderate reductions in S_{O_2}.

Journal of Experimental Biology

Journal of Experimental Biology (2017) 220, 531-536 doi:10.1242/jeb.149625

where β_b is the blood capacitance coefficient for O_2 or CO_2. The left part on the right-hand side of Eqn 17 corresponds to R_{perf} and simplifies to the normal perfusive resistance $[1/(1/2\dot{Q}_{tot}\beta_b)]$ when there are no shunts, whereas the right part is R_{vent}. The perfusive resistance (R_{perf}) can be expressed as the normal resistance without shunts ($R_{perf,F_{RL}=0}$) multiplied by a function of the shunt fraction [i.e. $f(F_{RL})=½(2-F_{RL})/(1-F_{RL})$]:

$$R_{tot} = R_{perf,F_{RL}=0} \cdot f(F_{RL}) + R_{vent}. \quad (18)$$

While R_{vent} is the same for O_2 and CO_2, R_{perf} and hence R_{tot} differ given different β_b. The gas exchange limitation (Piiper and Scheid, 1972, 1981) imposed by R–L shunts (L_{shunt}) is given by 1 minus the total resistance without shunts (R_{tot}, where $F_{RL}=0$) divided by the total resistance with shunts (i.e. R_{tot}):

$$L_{shunt} = 1 - \frac{R_{tot,F_{RL}=0}}{R_{tot}},$$
$$L_{shunt} = 1 - \frac{R_{perf,F_{RL}=0} + R_{vent}}{R_{perf,F_{RL}=0} \cdot f(F_{RL}) + R_{vent}}. \quad (19)$$

This can also be expressed by the dimensionless ratio of the normal perfusive to ventilatory resistance without shunts (φ):

$$L_{shunt} = 1 - \frac{\varphi + 1}{\varphi \cdot f(F_{RL}) + 1}, \quad (20)$$

where φ is given by the ventilation to perfusion ratio and the blood gas partitioning coefficient ($\lambda=\beta_b/\beta_g$) as follows:

$$\varphi = \frac{R_{perf,F_{RL}=0}}{R_{vent}} = \frac{\dot{V}_A}{½\dot{Q}_{tot}} \frac{1}{\lambda}. \quad (21)$$

From Eqn 20 it is given that the transport limitation imposed by shunts approaches zero when φ approaches zero (i.e. infinitely high blood flow and partitioning coefficient relative to ventilation). Conversely, the limitation approaches $F_{RL}/(2-F_{RL})$ when φ approaches infinity (i.e. infinitely high ventilation and low partitioning coefficient relative to blood flow).

RESULTS AND DISCUSSION

The isolated and combined effects of R–L shunts and ACR are illustrated in 3D plots in Fig. 1B–D, where arterial P_{CO_2}, P_{O_2} and HbO_2 saturation (S_{O_2}) are shown as functions of both R–L shunt fraction (F_{RL}) and alveolar ventilation. It is immediately clear that arterial P_{CO_2} increases most steeply when alveolar ventilation is reduced (i.e. reduced ACR), but only moderately when F_{RL} is increased (Fig. 1B). Conversely, both arterial P_{O_2} and S_{O_2} are markedly reduced as the R–L shunt increases, whilst reductions in alveolar ventilation only moderately reduce S_{O_2} (Fig. 1C,D). Thus, our theoretical analysis reveals substantial differences on the influence of R–L shunt and ACR on arterial blood gases, and predicts that ventilatory compensations are much more effective in altering arterial P_{CO_2} than cardiac shunt patterns.

The differences in the behaviours of O_2 and CO_2 upon changing shunt pattern or ACR are also illustrated in Fig. 2A–D, which shows P_{O_2}–P_{CO_2} diagrams and similar plots that relate P_{CO_2} and S_{O_2}. In Fig. 2B, the dashed line describes steady-state solutions for lung gases and hence also the arterial blood gases in the absence of cardiac shunts (i.e. the mammalian condition). In this case, reductions in ACR cause similar, but reciprocal changes in arterial P_{O_2} and P_{CO_2} as predicted by the respiratory quotient (RQ; set to 1 in the simulations). Conversely, an introduction of R–L shunt at a given ACR causes large reductions in arterial P_{O_2} while arterial P_{CO_2} only increases moderately (full green curve in Fig. 2B). Thus, to produce the same elevation in arterial P_{CO_2} by means of a R–L shunt as by a moderate reduction in ACR (e.g. a reduction from 28 to 20 ml air ml^{-1} CO_2; Fig. 2B), the shunt fraction would have to increase to 0.8, meaning that 80% of the systemic venous return bypasses the lungs (Fig. 2B). Such a large shunt fraction would concomitantly reduce arterial P_{O_2} from more than 120 mmHg to less than 30 mmHg (Fig. 2B) and reduce S_{O_2} from approximately 1.0 to less than 0.5 (Fig. 2A).

The complete solutions for different combinations of F_{RL} (varied 0–0.8) and ACR (varied 12.5–50) for arterial blood are given in Fig. 2C,D. The colour coding indicates increasing P_{CO_2} and the thicker lines originating from the air-line (the black dashed line/curve) depict how P_{O_2}, P_{CO_2} and S_{O_2} change as F_{RL} is altered at several constant levels of ACR. The thinner curves, originating from the thicker blood curves, represent solutions when ACR is altered at a given constant F_{RL}. By combining the horizontal axes of Fig. 2C, D, the possible solutions are summarized as a 3D diagram with P_{CO_2} on the vertical z-axis and S_{O_2} and P_{O_2} on the horizontal x- and y-axes (Fig. 2E). In this representation, the horizontal x–y plane reflects the effective O_2 equilibrium curve. Fig. 2E illustrates that increasing F_{RL} causes large reductions in P_{O_2} of the arterial and venous blood along the O_2 equilibrium curve, leading to pronounced S_{O_2} reduction with only moderate elevation of P_{CO_2}. Conversely, reducing ACR at a given F_{RL} leads to a large elevation of P_{CO_2} with only moderate reductions in S_{O_2} (thinner upwards-bending curves in Fig. 2E).

The different effects of altering ACR and R–L shunt on O_2 and CO_2 is explained by the differences in blood capacitance coefficients (β_b) (alternatively expressed as differences in blood

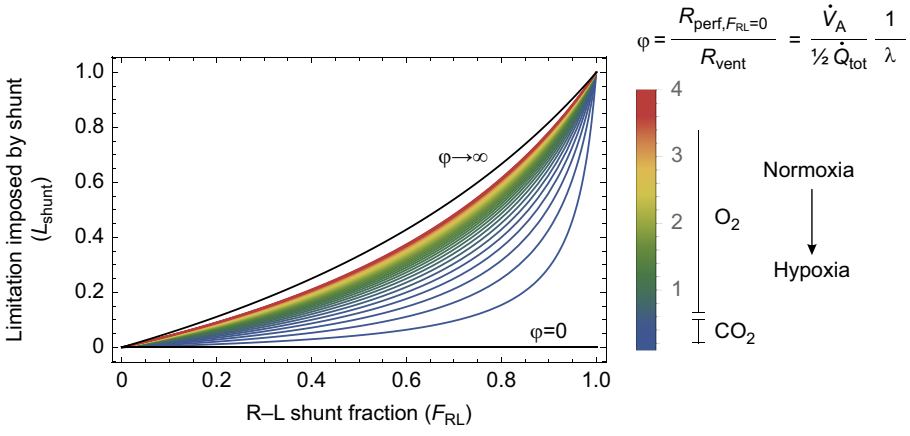

Fig. 3. Simplified analytic solution of the model that illustrates the limitation imposed on gas exchange by shunts (L_{shunt}, Eqn 21) as a function of the right-to-left shunt fraction (F_{RL}) for different values of the ratio of the perfusive to ventilatory resistance without shunts (φ, Eqn 22, colour coded). The asymptotic limitations when φ approaches infinity or zero are plotted. As a consequence of higher blood capacitance coefficient (β_b) and hence blood/gas partitioning coefficient (λ), φ for O_2 is higher than for CO_2 and hence O_2 uptake will be more limited by a given shunt.

gas partitioning coefficients, λ). This is illustrated in Fig. 3, showing the limitation imposed on gas exchange by F_{RL} (Eqn 21). Here, the ratio of the normal perfusive to ventilatory resistance without shunts (φ) is varied from a physiologically relevant range for O_2 and CO_2 (colour coded), and the asymptotic relationship between the limitation and F_{RL} for φ approaching infinity and φ=0 is given by the black curve and the horizontal axis. Fig. 3 emphasizes that at a given shunt fraction, the gas species mostly limited by the shunt is the one with the highest blood to air convective resistance (φ) and hence the lowest λ (i.e. lowest β_b). Therefore, owing to the high β_b, CO_2 is less limited by shunts than O_2, although the differences may become less distinct in deep hypoxia where the effective β_b for O_2 increases. The same conclusion was made by Wagner (1979) when considering the effects of lung shunts on O_2 versus CO_2 exchange. Besides the differences in effects of shunts on O_2 and CO_2, Fig. 3 also illustrates that the limitation in general is predicted to increase when overall $\dot{V}_A/\dot{Q}_{tot}$ is high and vice versa.

If digestion is facilitated by supplying the gut with blood with higher CO_2 levels, our model predicts that this is best mediated by reducing ACR instead of increasing R–L shunt. Elevating CO_2 levels by increasing R–L shunt would come at the cost of pronounced reductions in O_2 levels, producing hypoxemia at a time at which O_2 demand may be elevated fourfold above resting (e.g. Busk et al., 2000). Conversely, reductions of ACR entail much smaller reductions in O_2 delivery, but provide for an effective elevation of P_{CO_2} that compensates for the alkaline tide during digestion (Wang et al., 2001a). Furthermore, these postprandial reductions in ACR are well known in reptiles (Hicks et al., 2000; Overgaard et al., 1999; Secor et al., 2000) and P_{O_2} remains high during digestion in all animals studied, including alligators (Busk et al., 2000; Hartzler et al., 2006; Overgaard et al., 1999).

For many reptiles and amphibians, digestion is associated with large elevations in oxygen demands and an increased need to secrete gastric acid with resulting challenges to blood acid–base balance. Our theoretical approach clearly demonstrates that reliance on R–L shunting to meet the digestive demands conflicts significantly with increased metabolic demands of the digestive organs, and cannot provide adequate compensation for the alkaline tide. In contrast, ventilatory regulation, through reductions in ACR, addresses all the physiological challenges simultaneously, i.e. blood acid–base regulation, increased CO_2 delivery to the gastric mucosa without sacrificing O_2 delivery. Thus, while our theoretical model obviously does not provide information on the actual physiological responses of living animals, it would certainly seem that natural selection should favour efficient ventilatory regulation on arterial P_{CO_2} rather than the ineffective mean of regulation by central vascular shunts.

Competing interests
The authors declare no competing or financial interests.

Author contributions
This analysis results from numerous discussions over the past decade involving all the authors. C.L.M. constructed the model used in the manuscript on the basis of previous simpler attempts. The manuscript was written by H.M. and T.W. with continuous input and final approval of all co-authors.

Funding
This study was funded by the Danish Research Council (Natur og Univers, Det Frie Forskningsråd).

References
Busk, M., Overgaard, J., Hicks, J. W., Bennett, A. F. and Wang, T. (2000). Effects of feeding on arterial blood gases in the American alligator *Alligator mississippiensis*. *J. Exp. Biol.* **203**, 3117-3124.
Christoforides, C. and Hedley-Whyte, J. (1969). Effect of temperature and hemoglobin concentration on solubility of O_2 in blood. *J. Appl. Physiol.* **27**, 592-596.
Eme, J., Gwalthney, J., Blank, J. M., Owerkowicz, T., Barron, G. and Hicks, J. W. (2009). Surgical removal of right-to-left cardiac shunt in the American alligator (*Alligator mississippiensis*) causes ventricular enlargement but does not alter apnoea or metabolism during diving. *J. Exp. Biol.* **212**, 3553-3563.
Eme, J., Gwalthney, J., Owerkowicz, T., Blank, J. M. and Hicks, J. W. (2010). Turning crocodilian hearts into bird hearts: growth rates are similar for alligators with and without right-to-left cardiac shunt. *J. Exp. Biol.* **213**, 2673-2680.
Farmer, C. G., Uriona, T. J., Olsen, D. B., Steenblik, M. and Sanders, K. (2008). The right-to-left shunt of crocodilians serves digestion. *Physiol. Biochem. Zool.* **81**, 125-137.
Gardner, M. N., Sterba-Boatwright, B. and Jones, D. R. (2011). Ligation of the left aorta in alligators affects acid–base balance: a role for the R→ L shunt. *Respir. Physiol. Neurobiol.* **178**, 315-322.
Hartzler, L. K., Munns, S. L., Bennett, A. F. and Hicks, J. W. (2006). Metabolic and blood gas dependence on digestive state in the Savannah monitor lizard *Varanus exanthematicus*: an assessment of the alkaline tide. *J. Exp. Biol.* **209**, 1052-1057.
Hicks, J. W. (1998). Cardiac shunting in reptiles: mechanisms, regulation and physiological functions. *Biol. Reptilia* **19**, 425-483.
Hicks, J. W. and Wang, T. (2012). The functional significance of the reptilian heart: new insights into an old question. In *Ontogeny and Phylogeny of the Vertebrate Heart* (ed. T. Wang and D. Sedmera), pp. 207-227. New York: Springer-Verlag.
Hicks, J. W. and White, F. N. (1992). Pulmonary gas exchange during intermittent ventilation in the American alligator. *Respir. Physiol.* **88**, 23-36.
Hicks, J. W., Wang, T. and Bennett, A. F. (2000). Patterns of cardiovascular and ventilatory response to elevated metabolic states in the lizard *Varanus exanthematicus*. *J. Exp. Biol.* **203**, 2437-2445.
Jones, D. (1996). The crocodilian central circulation: reptilian or avian? *Verh. Dtsch. Zool. Ges.* **89**, 209-218.
Jones, D. R. and Shelton, G. (1993). The physiology of the alligator heart: left aortic flow patterns and right-to-left shunts. *J. Exp. Biol.* **176**, 247-270.
Monod, J., Wyman, J. and Changeux, J.-P. (1965). On the nature of allosteric transitions: a plausible model. *J. Mol. Biol.* **12**, 88-118.
Overgaard, J., Busk, M., Hicks, J. W., Jensen, F. B. and Wang, T. (1999). Respiratory consequences of feeding in the snake *Python molorus*. *J. Comp. Physiol. A* **124**, 359-365.
Piiper, J. and Scheid, P. (1972). Maximum gas transfer efficacy of models for fish gills, avian lungs and mammalian lungs. *Respir. Physiol.* **14**, 115-124.
Piiper, J. and Scheid, P. (1981). Model for capillary-alveolar equilibration with special reference to O_2 uptake in hypoxia. *Respir. Physiol.* **46**, 193-208.
Reeves, R. B. (1976). Temperature-induced changes in blood acid-base status: pH and P_{CO_2} in a binary buffer. *J. Appl. Physiol.* **40**, 752-761.
Secor, S. M., Hicks, J. W. and Bennett, A. F. (2000). Ventilatory and cardiovascular responses of a python (*Python molurus*) to exercise and digestion. *J. Exp. Biol.* **203**, 2447-2454.
Stewart, P. A. (1978). Independent and dependent variables of acid-base control. *Respir. Physiol.* **33**, 9-26.
Wagner, P. (1979). Susceptibility of different gases to ventilation–perfusion inequality. *J. Appl. Physiol.* **46**, 372-386.
Wang, T. and Hicks, J. W. (1996). The interaction of pulmonary ventilation and the right–left shunt on arterial oxygen levels. *J. Exp. Biol.* **199**, 2121-2129.
Wang, T., Busk, M. and Overgaard, J. (2001a). The respiratory consequences of feeding in amphibians and reptiles. *J. Comp. Physiol. A* **128**, 533-547.
Wang, T., Warburton, S., Abe, A. and Taylor, T. (2001b). Vagal control of heart rate and cardiac shunts in reptiles: relation to metabolic state. *Exp. Physiol.* **86**, 777-784.
Webb, G. J. (1979). Comparative cardiac anatomy of the Reptilia. III. The heart of crocodilians and an hypothesis on the completion of the interventricular septum of crocodilians and birds. *J. Morphol.* **161**, 221-240.
Weinstein, Y., Ackerman, R. A. and White, F. N. (1986). Influence of temperature on the CO_2 dissociation curve of the turtle *Pseudemys scripta*. *Respir. Physiol.* **63**, 53-63.

Journal of Experimental Biology